8.4 QUANTUM CALCULATIONS OF ENERGETICS OF RHENIUM CLUSTERS IN TUNGSTEN —

W. Setyawan, G. Nandipati, K. J. Roche, R. J. Kurtz (Pacific Northwest National Laboratory), and B. D. Wirth (University of Tennessee)

OBJECTIVE

The objective of this research is to explore the binding properties of small clusters of Re and intrinsic point defects in W. The results will be used to inform kinetic Monte Carlo simulations of radiation damage accumulation containing transmutant Re. In addition, the energetics and the forces will be used to develop an interatomic potential for the Re-W system.

SUMMARY

Density functional theory was employed to explore the energetic properties of clusters up to size 2 of Re in W. While WW<111> is the most stable intrinsic dumbbell, ReW<110> is more stable than ReW<111>. However, when they are trapped by a substitutional Re (Re_s), ReW<111> becomes more stable than ReW<110>. In this case, the most stable configuration forms a ReWRe crowdion with the W atom between the Re atoms. Simulations of a ReW[111] (dumbbell's vector is from Re to W) approaching a Re_s along [111] indicate that the binding energy decreases from 0.83 eV at the first nearest neighbor (NN1) to 0.10 eV at NN3 and ~0 at NN4. In addition, while ReW<111> and ReW<110> are stable near a Re_s at NN1, the ReW<100> instantaneously rotates toward ReW<111>.

PROGRESS AND STATUS

Method

VASP [1, 2] software was used to perform the quantum calculations within the density functional theory (DFT) framework. Core electrons are modeled with accurate projector-augmented-wave pseudopotentials [2]. Electrons at 6s and 5d states are treated as valence electrons for both W and Re. Perdew-Burke-Ernzerhof formulations [3] were employed for the exchange-correlation functionals. We used 250 eV as the energy cutoff for the plane waves. Defect energies were calculated using cubic 5x5x5 supercells of tungsten's bcc conventional unit cell. A Monkhorst-Pack grid of 3x3x3 was used to sample the k-points in the Brillouin zone [4]. The coordinates of atoms and the dimensions of the simulation cell were fully relaxed with a force tolerance of 0.025 eV/Å and an external pressure tolerance of 0.5 kbar. At the end of the relaxations, a static calculation was performed to eliminate errors due to basis incompleteness associated with changes in the simulation cell.

Results

Table 1 shows the formation energy of single point defects obtained in our calculations. The tungsten <111> dumbbell (WW<111>) is the most stable configuration for intrinsic dumbbells. The formation energy, E_f, of WW<111> is 9.97 eV. WW<110> is approximately 0.27 eV less stable than WW<111>. For ReW split dumbbells, ReW<110> is the most stable, E_f = 9.29 eV, which is also more stable than a WW<111>. However, ReW<111> is only 0.03 eV less stable than ReW<110>. Note that 0.03 eV is well above the total energy change in the last two ionic relaxations of < 1 meV. The effect of periodic images is negligible as will be demonstrated later. However, 0.03 eV may not be significant at high-temperature applications, especially if the rotation barrier between ReW<111> and ReW<110> is low. Nevertheless, it remains to be seen whether ReW<110> will still be more stable than ReW<111> in the presence of a substitutional Re (Re_s).

To explore the interaction between two point defects, we develop a utility code to enumerate all possible configurations and to reduce those configurations to a set of non-equivalent configurations. Figure 1 shows the numbering of the lattice sites that is used to generate the configurations. Sites 1, 2, 6, 7, 26, 27, 31, and 32 are the first nearest neighbors of site 126. Sites 7, 27, 31, 33, 37, and 57 are the second nearest neighbors of site 32. Sites 127, 131, 133, 137, 151, 153, 161, 163, 177, 181, 183, and 187 are the third nearest neighbors of site 157.

Table 1. Formation energy, E_f, of single point defects in tungsten calculated with 5x5x5 supercell of tungsten's bcc convectional unit cell.

Point defect	E_f (eV)
Vacancy	3.30
W <111> dumbbell	9.97
W <110> dumbbell	10.24
W <100> dumbbell	11.99
Substitutional Re	0.17
ReW <111> dumbbell	9.32
ReW <110> dumbbell	9.29
ReW <100> dumbbell	11.28

First, we explore the binding between Re_s and ReW<111> and between Re_s and ReW<110> at the first nearest neighbor (NN1) distance. There are four unique configurations for the former, and three unique configurations for the latter. Note that the vector from Re to W in the dumbbell is taken as the direction of the dumbbell. The binding energies (E_b) are summarized in Table 2. As usual, a positive value indicates attraction. While some of the calculations are still running, it appears that ReW<111> (E_b = 0.83 eV) becomes more stable than ReW<110> (E_b = 0.53 eV) when it is trapped by a Re_s at NN1 distance. With Re_s at site 126, the most stable configuration is ReW[111] at site 1, forming a ReWRe crowdion. Exploration of the binding energies at NN2 distance is underway. While ReW<111> and ReW<110> are stable near Re_s at NN1, ReW<100> instantaneously transforms into ReW<111>.

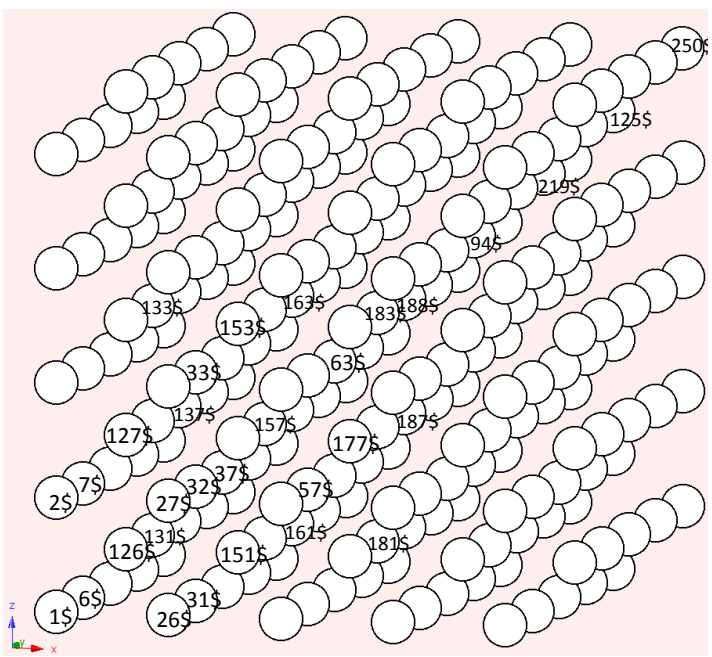

Figure 1. Numbering of lattice sites in the 5x5x5 supercell. Sites 1, 2, 6, 7, 26, 27, 31, and 32 are the first nearest neighbors of site 126. Sites 7, 27, 31, 33, 37, and 57 are the second nearest neighbors of site 32. Sites 127, 131, 133, 137, 151, 153, 161, 163, 177, 181, 183, and 187 are the third nearest neighbors of site 157.

Table 2. Binding energy, E_b, between a substitutional Re and a ReW<111> or a ReW<110> dumbbell. The i and j denotes the location of the first and second point defect, respectively, and corresponds to the numbering of sites as shown in Figure 1. The vector from the Re to the W atom in the dumbbell is taken as the direction of the dumbbell. R indicates that full relaxation has not been reached (simulations still in progress).

Substitutional Re	ReW<111>	E_b (eV)
i-126	j-1 [111] j-1 [11-1] j-1 [1-1-1] j-1 [-1-1-1]	0.83 0.54 R 0.45 R 0.60 R
Substitutional Re	ReW<111>	E_b (eV)
i-126	j-1 [110] j-1 [1-10] j-1 [-1-10]	0.53 -0.03 R 0.47 R

To estimate the range of the interaction between the Re_s and a ReW<111>, we separate them along a specific direction, [111], up to the fifth neighbor (the maximum distance allowed with the 5x5x5 supercell). At this moment, two permutations of the dumbbell vector have been completed, namely ReW[111] and ReW[-1-1-1]. For the ReW[111], the dumbbell approaches the Re_s along [111]. The E_b decreases from 0.83 eV at NN1 to 0.10 eV at NN3 and ~0 at NN4. While for the ReW[-1-1-1], it approaches the Re_s along [-1-1-1]. The E_b decreases from 0.60 eV at NN1 to 0.01 eV at NN3 and ~0 at NN4. The results are summarized in Table 3. These results also indicate that the effect of periodic images is negligible.

Table 3. Binding energy, E_b, between a substitutional Re and a ReW[111] or a ReW[-1-1-1] dumbbell separated along [111]. NNn denotes that they are separated at the n-th nearest neighbor along [111]. The i and j denotes the location of the first and second point defect as shown in Figure 1. The vector from the Re to the W atom in the dumbbell is taken as the direction of the dumbbell.

Substitutional Re	ReW[111]	E_b (eV)
i-126	j-1 NN1 j-250 NN2 j-125 NN3 j-219 NN4 j-94 NN5	0.83 0.61 0.10 ~0 ~0
Substitutional Re	ReW[-1-1-1]	E_b (eV)
i-126	j-32 NN1 j-157 NN2 j-63 NN3 j-188 NN4	0.60 0.13 0.01 ~0

Next, we explore the binding between two dumbbells, namely two ReW<111>, two ReW<110>, and between ReW<111> and ReW<110>. Table 4 -Table 6 summarize the enumeration of the non-equivalent configurations for these dumbbells separated up to NN2. Most of the calculations are still underway as indicated by missing entries.

Table 4. Non-equivalent configurations between two ReW<111> separated at the first (top panel) and second (bottom panel) nearest neighbor distance. Site-i and site-j indicates the location of the first and second dumbbell, respectively. The numbering of the sites is shown in Figure 1. R indicates that full relaxation has not been reached.

Configuration	First dumbbell	Second dumbbell	E_b (eV)
1	i-126 [111]	j-1 [111]	2.10
2	i-126 [111]	j-1 [11-1]	5.50 R
3	i-126 [111]	j-1 [1-1-1]	5.62 R
4	i-126 [111]	j-1 [-1-1-1]	1.47
5	i-126 [111]	j-2 [111]	6.35 R
6	i-126 [111]	j-2 [11-1]	5.66 R
7	i-126 [111]	j-2 [1-11]	5.74 R
8	i-126 [111]	j-2 [1-1-1]	4.67 R
9	i-126 [111]	j-2 [-1-1-1]	6.23 R
10	i-126 [111]	j-7 [11-1]	5.12 R
11	i-126 [111]	j-7 [1-1-1]	5.83 R
12	i-126 [111]	j-7 [-1-1-1]	6.44 R
13	i-126 [111]	j-32 [-1-1-1]	2.63
1	i-32 [111]	j-7 [111]	
2	i-32 [111]	j-7 [11-1]	
3	i-32 [111]	j-7 [-111]	
4	i-32 [111]	j-7 [1-1-1]	
5	i-32 [111]	j-7 [-11-1]	
6	i-32 [111]	j-7 [-1-1-1]	
7	i-32 [111]	j-33 [11-1]	
8	i-32 [111]	j-33 [1-1-1]	
9	i-32 [111]	j-33 [-1-1-1]	

Table 5. Non-equivalent configurations between two ReW<110> separated at the first (top panel) and second (bottom panel) nearest neighbor distance. Site-i and site-j indicates the location of the first and second dumbbell, respectively. The numbering of the sites is shown in Figure 1. R indicates that full relaxation has not been reached.

Configuration	First dumbbell	Second dumbbell	E_b (eV)
1	i-126 [110]	j-1 [110]	6.12 R
2	i-126 [110]	j-1 [1-10]	5.65 R
3	i-126 [110]	j-1 [-1-10]	5.98 R
4	i-126 [110]	j-1 [101]	3.85 R
5	i-126 [110]	j-1 [10-1]	5.36 R
6	i-126 [110]	j-1 [-101]	5.35 R
7	i-126 [110]	j-1 [-10-1]	3.61 R
8	i-126 [110]	j-6 [110]	6.02 R
9	i-126 [110]	j-6 [1-10]	5.78 R
10	i-126 [110]	j-6 [-1-10]	6.05 R
11	i-126 [110]	j-6 [101]	5.41 R
12	i-126 [110]	j-6 [10-1]	5.61 R
13	i-126 [110]	j-6 [-101]	5.62 R
14	i-126 [110]	j-6 [0-11]	5.38 R
15	i-126 [110]	j-31 [-1-10]	6.16 R
16	i-126 [110]	j-31 [-101]	3.68 R
1	i-32 [110]	j-7 [110]	
2	i-32 [110]	j-7 [1-10]	
3	i-32 [110]	j-7 [-110]	
4	i-32 [110]	j-7 [-1-10]	
5	i-32 [110]	j-7 [101]	
6	i-32 [110]	j-7 [-101]	
7	i-32 [110]	j-7 [011]	
8	i-32 [110]	j-7 [0-11]	
9	i-32 [110]	j-31 [110]	
10	i-32 [110]	j-31 [1-10]	
11	i-32 [110]	j-31 [-1-10]	
12	i-32 [110]	j-31 [101]	
13	i-32 [110]	j-31 [-101]	
14	i-32 [110]	j-37 [1-10]	
15	i-32 [110]	j-37 [-1-10]	
16	i-32 [110]	j-37 [0-11]	

Table 6. Non-equivalent configurations between ReW<111> and ReW<110> separated at the first (top panel) and second (bottom panel) nearest neighbor distance. Site-i and site-j indicates the location of the first and second dumbbell, respectively. The numbering of the sites is shown in Figure 1.

Configuration	First dumbbell	Second dumbbell	E_b (eV)
1	i-126 [111]	j-1 [110]	
2	i-126 [111]	j-1 [1-10]	
3	i-126 [111]	j-1 [-1-10]	
4	i-126 [111]	j-2 [110]	
5	i-126 [111]	j-2 [1-10]	
6	i-126 [111]	j-2 [-1-10]	
7	i-126 [111]	j-2 [101]	
8	i-126 [111]	j-2 [10-1]	
9	i-126 [111]	j-2 [-101]	
10	i-126 [111]	j-2 [-10-1]	
11	i-126 [111]	j-7 [110]	
12	i-126 [111]	j-7 [1-10]	
13	i-126 [111]	j-7 [-110]	
14	i-126 [111]	j-7 [-1-10]	
15	i-126 [111]	j-7 [011]	
16	i-126 [111]	j-7 [01-1]	
17	i-126 [111]	j-7 [0-1-1]	
18	i-126 [111]	j-32 [110]	
19	i-126 [111]	j-32 [1-10]	
20	i-126 [111]	j-32 [-1-10]	
1	i-32 [111]	j-7 [110]	
2	i-32 [111]	j-7 [1-10]	
3	i-32 [111]	j-7 [-110]	
4	i-32 [111]	j-7 [-1-10]	
5	i-32 [111]	j-7 [011]	
6	i-32 [111]	j-7 [01-1]	
7	i-32 [111]	j-7 [0-1-1]	
8	i-32 [111]	j-33 [110]	
9	i-32 [111]	j-33 [1-10]	
10	i-32 [111]	j-33 [-1-10]	
11	i-32 [111]	j-33 [101]	
12	i-32 [111]	j-33 [10-1]	
13	i-32 [111]	j-33 [-101]	
14	i-32 [111]	j-33 [-10-1]	

This research has been supported by the U.S. Department of Energy, Office of Science, and Office of Fusion Energy Sciences (DE-AC06-76RL0-1830).

References

[1] P. E. Blöchl, Phys. Rev. B 50 (1994) 17953.
[2] G. Kresse and D. Joubert, Phys. Rev. B 59 (1999) 1758.
[3] J. P. Perdew, K. Burke and M. Ernzerhof, Phys. Rev. Lett. 77 (1996) 3865.
[4] H. J. Monkhorst and J. D. Pack, Phys. Rev. B 13 (1976) 5188.